1
2 Running head: River metabolism and carbon spiraling
3
4
5
6 **Metabolism, gas exchange, and carbon spiraling in rivers**
7
8

9 Robert O. Hall, Jr.
10 Department of Zoology and Physiology, University of Wyoming, Laramie, Wyoming,
11 82071, USA
12
13 Jennifer L. Tank
14 Department of Biological Sciences, University of Notre Dame, Notre Dame, Indiana
15 46556, USA
16
17 Michelle A. Baker
18 Department of Biology and Ecology Center, Utah State University, Logan, Utah 84322,
19 USA
20
21 Emma J. Rosi-Marshall
22 Cary Institute of Ecosystem Studies, Box AB, Millbrook, New York, 12545, USA
23
24 Erin R. Hotchkiss
25 Program in Ecology and Department of Zoology and Physiology, University of
26 Wyoming, Laramie, Wyoming, 82071, USA
27
28 Current address: Department of Ecology and Environmental Science, Umeå University,
29 90187, Umeå, Sweden
30
31
32
33
34 ROH designed the study, conducted fieldwork, analyzed data, and wrote first draft of the
35 paper. JLT, MAB, and EJR-M designed the study, conducted fieldwork, and wrote the
36 paper. ERH conducted field and lab work and wrote the paper.
37
38
39
40
41
42
43
44
45
46

Abstract

Ecosystem metabolism, i.e., gross primary productivity (GPP) and ecosystem respiration (ER), controls organic carbon (OC) cycling in stream and river networks and is expected to vary predictably with network position. However, estimates of metabolism in small streams outnumber those from rivers such that there are limited empirical data comparing metabolism across a range of stream and river sizes. We measured metabolism in 14 rivers (discharge range 14 to 84 m^3 s^{-1}) in the Western and Midwestern United States (US). We estimated GPP, ER, and gas exchange rates using a Lagrangian, 2-station oxygen model solved in a Bayesian framework. GPP ranged from 0.6 to 22 g O_2 m^{-2} d^{-1} and ER tracked GPP, suggesting that autotrophic production supports much of riverine ER in summer. Net ecosystem production, the balance between GPP and ER was 0 or greater in 4 rivers showing autotrophy on that day. River velocity and slope predicted gas exchange estimates from these 14 rivers in agreement with empirical models. Carbon turnover lengths (i.e., the distance traveled before OC is mineralized to CO_2) ranged from 38-1190 km, with longest turnover lengths in high-sediment, arid-land rivers. We also compared estimated turnover lengths with the relative length of the river segment between major tributaries or lakes; the mean ratio of carbon turnover length to river length was 1.6, demonstrating that rivers can mineralize much of the OC load along their length at baseflow. Carbon mineralization velocities ranged from 0.05 to 0.81 m d^{-1}, and were not different than measurements from small streams. Given high GPP relative to ER, combined with generally short OC spiraling lengths, rivers can be highly reactive with regard to OC cycling.

2

69   Key words: rivers, gross primary production, ecosystem respiration, carbon spiraling, gas

70   exchange, ecosystem metabolism

71

72   **Introduction**

73   There is a renewed interest in carbon cycling in freshwater ecosystems as

74   ecologists link metabolic processes with regional carbon (C) budgets (Battin and others

75   2009; Tranvik and others 2009), but empirical measurements of metabolism in a wide

76   variety of freshwater ecosystems are lacking, as is our understanding of processes that

77   control variation within and across ecosystems. Ecosystem size and position in the

78   landscape will control variation in rates of C supply and *in situ* metabolism; for example,

79   lake size correlates with metabolism (Staehr and others 2012). In the case of streams and

80   rivers, ecosystem processes such as C cycling will vary both as a function of size (as

81   volumetric flow) and landscape position, given that the downstream movement of water

82   connects headwaters with larger streams and rivers (Webster 2007). The effects of stream

83   size and landscape position on C cycling were initially conceptualized as part of the River

84   Continuum Concept (RCC) where headwater streams were predicted to have high rates of

85   ecosystem respiration (ER) relative to gross primary production (GPP), whereas mid-order

86   reaches were predicted to have higher GPP relative to ER because of increased light

87   availability supporting autochthony combined with reduced allochthonous inputs of C

88   (Vannote and others 1980). In contrast, large rivers with high sediment loads would revert

89   to a pattern of higher ER relative to GPP, like headwater streams, because of decreased

90   light penetration in the water column combined with the import of allochthonous particles

91   from upstream. Data from selected river continua have supported the pattern of increasing

92 GPP/ER downstream from headwaters to non-wadeable rivers (Meyer and Edwards 1990;

93 McTammany and others 2003).

94   Despite strong conceptual foundations and limited empirical data on how larger

95 streams and rivers function, metabolism estimates in rivers are far fewer in number than

96 those from small streams. Only 10% of reach-scale metabolism estimates (reviewed

97 below) have been conducted in rivers with discharge >10 m^3 s^{-1} (~20 m width), while >

98 50% have been made in streams < 0.1 m^3 s^{-1}. Recent advances for estimating gas

99 exchange from dissolved oxygen (O_2) data (Holtgrieve and others 2010; Dodds and

100 others 2013) make estimating metabolism in rivers potentially as straightforward as in

101 small streams. In addition, understanding variation and controls on metabolism in rivers

102 will allow ecologists to answer a variety of unanswered questions in river networks. For

103 example, river food webs are based to a large degree on *in situ* primary production

104 (Thorp and Delong 2002; Cross and others 2013), but there are few data on the actual

105 rates of primary production in rivers.

106   More broadly, ecosystem metabolism in rivers is of general interest because of the

107 potential for rivers to store, mineralize, and transport terrestrial organic carbon (OC)

108 before reaching the coastal zone (Battin and others 2008; Raymond and others 2013). It is

109 well known that small streams can respire large quantities of terrestrial OC (Marcarelli

110 and others 2011), yet the role of rivers is less understood, despite evidence showing that

111 big rivers also transform terrestrial OC (Cole and Caraco 2001). Riverine metabolism

112 estimates will also facilitate the calculation of OC spiraling lengths (Newbold and others

113 1982), allowing further comparison among small streams and larger rivers. The OC

114 spiraling method examines downstream C flux relative to mineralization and is a direct

4

115 estimate of the degree to which rivers mineralize versus transport OC. Oddly, ecosystem

116 ecologists rarely use this spiraling metric to describe the role of streams and rivers in C

117 cycling despite strong theoretical (Webster 2007) and empirical (Thomas and others

118 2005; Taylor and others 2006; Griffiths and others 2012) examples.

119   Here, we measured metabolism of 14 rivers ranging in size from 14 to 84 $m^{-3}\ s^{-1}$

120 to link metabolism metrics with OC cycling. We had 3 objectives: 1) develop a two-

121 station model, solved via Bayesian inverse modeling of metabolism parameters, to

122 measure metabolism in each of 14 rivers varying in physical attributes in Midwest and

123 Western US; 2) combine riverine metabolism values with others from the literature to

124 examine how the balance of GPP and ER varies across a large size range of streams and

125 rivers; and 3) calculate instantaneous metrics of OC spiraling to estimate the degree to

126 which river reaches can process OC.

127

128 **Methods**

129 *Study sites*

130   We chose 14 rivers in the Midwest and Western US that varied chemically,

131 physically, and geomorphically (Table 1, Appendix 1). This study was part of a larger

132 study investigating nutrient cycling in rivers, thus we chose sites to maximize variation in

133 suspended sediment and nutrient concentrations. Sites in western Wyoming and eastern

134 Idaho had low nutrient and low suspended sediment concentrations, central Wyoming

135 and Utah rivers had low to medium nutrient concentrations and medium to high

136 suspended sediments, and Midwestern rivers had generally higher nutrients and low to

137 medium suspended sediments (Table 1). We chose the study reaches by taking in to

138   consideration the proximity of bridges for adding solutes, the presence of USGS gages

139   for measurements of discharge, and the presence of boat ramps for reach-scale sampling

140   logistics. Rivers varied in summer baseflow discharge from 14 to 84 $m^3 s^{-1}$ with an

141   average of 39 $m^3 s^{-1}$.

142

143   *Field and laboratory methods*

144   At most sites we performed two-station metabolism estimates based on sampling

145   dissolved O_2 through time. To measure dissolved O_2 we anchored 2-4 multi-parameter

146   Hydrolab Minisondes equipped with optical O_2 sensors in areas of moderate downstream

147   flow, at stations 2.5-10.7 km apart (mean 6.1 km) along each river, with mean distance

148   between sondes corresponding to an average of 2.7 h of travel time. We calibrated the

149   sondes river-side in a 100-L pot of air-saturated water that we vigorously bubbled using

150   an aquaculture air pump and air stone. This method of bubbling oversaturates O_2 by 2%.

151   Bubbling this pot in the laboratory and measuring Ar (which has similar diffusivity as O_2)

152   on a membrane-inlet mass spectrometer, we found that Ar was 2% (±0.15%)

153   oversaturated. This phenomenon is likely due to oversaturation due to bubble-mediated

154   gas exchange (e.g., Hall et al. 2012).   We corrected our oxygen data downwards by 2%

155   to counter this over calibration. Following initial calibration, we recorded O_2 readings in

156   this air saturated water to check calibration and that all sondes remained within 2% of

157   saturation; O_2 readings from sondes drifted little during the deployments and thus did not

158   need drift correction. We recorded O_2, temperature, and turbidity using these sondes at

159   5-min intervals during 3-d deployments during summer baseflow conditions (i.e., July or

160   August).

161   We also collected physical and chemical data at each site; discharge (Q, m^3 s^{-1})

162   came from nearby USGS gaging stations or gages associated with upstream dams. We

163   measured wetted channel width (w, m) of the reach at ~70 locations throughout the study

164   reach using a laser rangefinder operated from a boat. We also conducted solute tracer

165   additions as part of nutrient uptake experiments, adding Rhodamine WT (RWT) and

166   NaBr in separate pulse additions with target downstream concentrations of 10 µg RWT L^-

167   ^{1} or 50 µg Br^- L^{-1}. We monitored RWT at 4 stations downstream of the release point

168   using 4 Hydrolab Minisondes equipped with fluorometric sensors programmed to record

169   RWT concentration every 10 seconds while Br^- samples were manually collected from

170   the river thalweg at timed intervals and analyzed using ion chromatography (Dionex

171   models ICS-5000) using US-EPA standard method 300.0. These tracer releases were

172   used to calculate nominal travel time (i.e., the time for 50% of the solute to pass the

173   downstream station), and mean velocity (V, m min^{-1}) was then calculated as reach

174   length/nominal travel time, while mean depth (z, m) was estimated based on continuity, z

175     $= Q/(wV)$. We also measured background water column nutrients at each site as part of

176   the nutrient uptake experiments and reach-scale estimates were based on the average of 3

177   to 5 samples collected at 4 sites. We analyzed NH_4^+-N using the phenol-hypochlorite

178   method (Solorzano 1969), NO_3^--N using the cadmium reduction method (APHA 1995)

179   and SRP using the ascorbic acid method (Murphy and Riley 1962) on a Lachat Flow

180   Injection Autoanalyzer (Lachat Instruments, Loveland, CO, USA).

181   To estimate C spiraling, we sampled particulate OC (POC) and dissolved OC

182   (DOC). We collected POC from 3 grab samples taken in the thalweg at 4 locations from

183   each river. Rivers averaged 0.6 to 1.3 m deep and were turbulent; hence, we did not take

184   depth-integrated samples.   For POC, we immediately filtered a known volume of water

185   in the field onto pre-ashed and weighed glass fiber filters (Whatman GF/F), air died the

186   filters and stored them for transport to the lab where we dried them at 60°C, weighed

187   them, and combusted at 500°C. We reweighed the filters to obtain an ash-free dry mass

188   (AFDM) and converted to mg AFDM/L given the volume of sample filtered; we assumed

189   that 50% 0f AFDM was C. Samples for DOC came from triplicate samples at one

190   location. These were filtered with pre-ashed glass fiber filters (Whatman GF/F), acidified

191   with HCl to a pH of 2, and then stored in acid washed and ashed borosilicate amber vials

192   (I-Chem, 40mL). We transported samples on ice to the laboratory, and refrigerated them

193   until analysis on a Shimadzu Total Organic Carbon Analyzer (TOC-5000A; measurement

194   precision of $\pm$ 0.05 mg C L^{-1}).

195

196   *Metabolism estimation*

197   We estimated metabolism and gas exchange by fitting a two-station Lagrangian

198   model to the dissolved O$_2$ data, except for the Muskegon, North Platte, and Bear rivers

199   where we used a one-station method due to instrument failures or burial of the upstream

200   sondes. A two-station procedure measures metabolism in a defined reach of river

201   between the upstream and downstream O$_2$ sensors, which allows estimation of reach-

202   scale metabolism, even below river discontinuities, such as dams, which may be included

203   in the upstream footprint of one-station O$_2$ measurements. A general model for two-

204   station metabolism is:

205         $Odown_{(t+\tau)} = Oup_{(t)} + GPP + ER + gas\ exchange$

206   (1)

207 where $Oup_{(t)}$ is the upstream O_2 concentration (g O_2 m^{-3}) and $Odown_{(t+\tau)}$ is downstream

208 O_2 concentration of that same parcel of water following travel time, τ. GPP and ER are

209 both expressed in g O_2 m^{-2} d^{-1}, and represented as positive and negative rates of O_2

210 production and consumption, respectively.

211   An expansion of this model is:

$$Odown_{(t+\tau)} = Oup_{(t)} + \left(\frac{GPP}{z} \times \frac{\sum_t^{t+\tau} PPFD}{PPFD_{total}}\right) + \frac{ER}{z}\tau$$

$$+ K\tau\left(\frac{Osatup_{(t)} + Osatdown_{(t+\tau)}}{2} - \frac{Oup_{(t)} + Odown_{(t+\tau)}}{2}\right)$$

212 (2)

213 where z is mean depth (m), $Osatup$ and $Osatdown$ are O_2 saturation concentrations

214 upstream and downstream (g O_2 m^{-3}). Gas exchange flux was the gas exchange rate, K

215 (d^{-1}) multiplied by the dissolved O_2 saturation deficit, which we averaged for the

216 upstream and downstream stations. We use light to drive GPP in this model (Van de

217 Bogert and others 2007). For any parcel of water, the fraction of light it accumulates is

218 the sum of the photosynthetic photon flux density (PPFD, μmol m^{-2} s^{-1}) accumulated in

219 the time interval from t to $(t + \tau)$ divided by the daily total of PPFD ($PPFD_{total}$). Equation

220 2 has $Odown$ on both sides; we need $Odown$ on the left side of the equation because we

221 are comparing modeled $Odown$ with the data. Following some algebra we get:

222

$$Odown_{(t+\tau)}$$

$$= \frac{Oup_{(t)} + \left(\frac{GPP}{z} \times \frac{\sum_t^{t+\tau} PPFD}{PPFD_{total}}\right) + \frac{ER}{z}\tau + K\tau\left(\frac{Osatup_{(t)} - Oup_{(t)} + Osatdown_{(t+\tau)}}{2}\right)}{1 + \frac{K\tau}{2}}$$

223   (3)

224   Assumptions of this model are that GPP is a linear function of light intensity, ER

225   is constant throughout the day, and that the average of up and down station O_2 saturation

226   deficit is representative for the entire reach. We tested the assumption of linear light

227   relationships by using 1-station models (equation 4 below) for 1 day on each river with a

228   Jassby-Platt light saturation function exactly following Holtgrieve and others (2010).

229   Eight of 14 rivers had linear light response curves. Six showed slightly curvilinear

230   relationships, with increase in GPP 3-10%, with a concomitant two-fold increase in the

231   credible intervals. In a two-station model with 3-h travel times, it would be necessary to

232   divide these travel times into 5-min intervals to calculate and sum GPP for each. We felt

233   that a potential increase in accuracy of 10% for 6 of the rivers did not warrant this

234   increased model complexity. We did not include a diel temperature response for ER

235   because the relationship of ER to temperature is highly variable (Huryn and others 2014,

236   Jankowski and others 2014), and thus we would have needed to estimate this parameter

237   in addition to GPP, ER, and K, possibly producing an overfitted model. Gas exchange is

238   estimated as K_{600} (d^{-1}) and is corrected for temperature at each time step based on

239   Schmidt number scaling (Jähne and Haußecker 1998). We convert this per time rate to a

240   gas exchange velocity ($k_{600,}$ m/d) by multiplying by mean depth, z, to facilitate

241   comparisons with published gas exchange velocities. We used modeled solar insolation

242   data for Eq 3 based on geographic location and time of day and year.

243   For the 3 rivers using a one station method (North Platte, Bear, and Muskegon),

244   we used the following model (Van de Bogert and others 2007):

245    $$O_t = O_{t-\Delta t} + \frac{GPP}{z} \times \frac{PPFD_t}{PPFD_{total}} + \frac{ER}{z} \Delta t + K \Delta t (Osat_{t-\Delta t} - O_{t-\Delta t}) \qquad (4)$$

246

247   where t is time of day and Δt is the time between O_2 measurements. This model measures

248   O_2 change in one place rather than tracking it downstream and in a longitudinally

249   homogenous river, one-station analyses will give the similar results to a two-station

250   model (Reichert and others 2009). Of the 3 rivers, only the Muskegon had a dam located

251   47 km upstream, but we suggest that its influence was negligible because the dam was

252   located twice the distance ($1.6V/K$) for 80% of O_2 turnover (Chapra and Di Toro 1991) .

253   Based on the above models, we used a Bayesian inverse modeling procedure to

254   estimate metabolism (GPP and ER) and gas exchange rate (K_{600}) roughly following

255   Holtgrieve and others (2010). Bayesian analysis treats parameters as random variables

256   with a corresponding probability distribution and allows estimating uncertainty for the

257   modeled parameters. Because we solved for gas exchange as well as GPP and ER, there

258   is the risk of overfitting the model, and posterior probability distributions solved via a

259   Bayesian approach allowed us to examine this assumption closely. At all but one sites we

260   had two full days of data, and we fit each daytime period separately starting at 22:00 the

261   night before to 06:00 the day after for a total of 32 h.

262   Following Bayes rule, we calculated the posterior probability distribution of the

263   parameters as:

264         $$P(\theta \,|\, D) \propto P(D \,|\, \theta) \times P(\theta) \tag{5}$$

265   where θ is a vector of parameters, GPP, ER and K, and D is the O_2 data for the

266   downstream or single station. The likelihood of the data given θ assumes normally

267   distributed error and is calculated as:

268         $$\mathcal{L}(D|\theta) = \prod_{i=1}^{n} N(D_i | \mu_i, \sigma_i^2) \tag{6}$$

269   where the likelihood of D given θ is the product of likelihoods of the data relative to

270   modeled downstream O_2 concentrations (μ_i,) and variance (σ_i^2) . We simulated the

271   posterior distribution $P(\theta\,|D)$ using a Metropolis algorithm and Markov-chain Monte

272   Carlo (MCMC) using function *metrop* in the *mcmc* package for R (Geyer 2010, R

273   Development Core Team 2011). We ran each chain for 20,000 iterations following burn

274   in and we started all MCMC chains with different parameter values to ensure a global

275   solution. We did not thin chains and we adjusted the proposal distribution of the

276   Metropolis algorithm to achieve an acceptance rate near 20%. For metabolism

277   parameters, we used minimally informative prior probability distributions (GPP $\sim N$

278   (μ=5, sd=10), ER $\sim N$ (μ=-5, sd=10). For gas exchange, we used the nighttime regression

279   method (Hornberger and Kelly 1975) or empirical equation 7 from Raymond and others

280   (2012) to assign a normal prior probability distribution, where the mean and standard

281   deviation of the prior probability distribution were the mean and standard deviation

282   respectively of the 4 slopes from nighttime regression measured by the two O_2 sondes

283   over two nights or the error in the predictive equation. Code for one- and two-station

284   models is in Appendix 5.

285

286   *Calculation of C spiraling*

287   We calculated turnover length of OC for each river following (Newbold and others 1982)

288   where spiraling length (S_{OC}, m) is the ratio of downstream transport relative to

289   mineralization and is calculated as:

290         $$S_{OC} = \frac{Q \times [OC]}{-HR \times w} \qquad\qquad (7)$$

291

292   Discharge (Q) and stream width (w) were estimated as described above, and the sum of

293   POC and DOC gives the organic C concentration [OC]. However, to calculate S_{OC}

294   requires an estimate of heterotrophic respiration (HR, which is a negative flux) that

295   equals ER – AR, where AR is the respiration by algae and macrophytes themselves.

296   Typically researchers assume that AR is some fraction of GPP (e.g., 0.2 to 0.5) but a

297   recent analysis suggests that the daily fraction of GPP (AR_f) consumed by respiration by

298   algae is about 44% (Hall and Beaulieu 2013). Assuming this fraction, we estimated HR

299   as:

300    $$HR = ER - AR_f \times GPP \qquad (8)$$

301   Turnover length of OC will depend strongly of the size of the river. To compare

302   mineralization relative to [OC] (i.e., [DOC] + [POC]) we calculated a "mineralization

303   velocity" ($v_{f\text{-}OC}$, m d^{-1}) of OC as:

304    $$v_{f-oc} = \frac{-HR}{[OC]} \qquad (9)$$

305   analogous to uptake velocity measured in nutrient uptake studies (Hall and others 2013).

306   We converted HR in O$_2$ units to g C m^{-2} d^{-1} by assuming a 1:1 molar relationship between

307   C and O in respiration and we then compared $v_{f\text{-}OC}$ to those measured in other rivers and

308   streams where OC spiraling length was reported. Error in not perfectly knowing AR_f may

309   introduce error into estimates of $v_{f\text{-}OC}$. Therefore we calculated $v_{f\text{-}OC}$ 1000 times with

310   each replicate using a randomly selected estimate of AR_f from Hall and Beaulieu (2013)

311   and 3 subsequent studies (Roley and others 2014, Genzoli and Hall in revision, R. O.

312   Hall et al, unpublished data). Finally, we compared Soc to the estimate of river length

313   estimated from GIS; we defined the segment distance for each river as the length of river

314   downstream of a major reservoir or confluence of large tributary and upstream of a lake,

315   reservoir, or much larger river. This designation of river length was not meant as a

316   definition, but rather to provide some context for considering OC turnover length, *Soc*.

317

318   *Statistical inference*

319   We used Pearson correlations to relate rates of metabolism to predictor variables,

320   and rates of C spiraling to river size. Inference on this correlation coefficient (*r*) was

321   based on calculating default Bayes factors for correlation (Wetzels and Wagenmakers

322   2012), which can be interpreted as the relative probability that a linear relation exists

323   between 2 variables. Bayes factors >6 constitute strong evidence in support of the

324   alternative hypothesis (linear relation) versus a null.   We estimated error on metabolism

325   estimates, GPP, ER and K_{600}, not as the parameter error from the MCMC solutions, but

326   rather on the bootstrap 95% confidence intervals from the 2-8 metabolism estimates (i.e.,

327   the median value of the posterior probability distributions) at each site. This approach

328   assumes no within-estimate error, which follows the fact that the among-estimate error

329   exceeded the parameter error from any one MCMC solution. We performed all statistics

330   using R (R Development Core Team 2011).

331   We compared rates of metabolism in this study to those from many other streams

332   and rivers, collating estimates of reach-scale, open channel metabolism from Marcarelli

333   and others (2011). We also added newer studies to this data set, of which several are

334   from similar sized rivers as the ones studied here (Appendix 4). We used locally

335   weighted regression (Trexler and Travis 1993) with a smoothing parameter of 0.75 to

336   visualize trends in metabolism as a function of river discharge.

337

338 **Results**

339   Models fit the data closely and had low error in estimates of the parameters, GPP,

340 ER, and K (Fig 1). The 95% credible interval on metabolism parameters for any model

341 fit averaged < 10% of the of value of the parameter itself (Table 1). Variation in

342 parameter estimates between the two measurement days or among sondes was higher

343 than credible intervals within any one day (Table 1, Appendix 2).

344   GPP and ER varied strongly among the 14 rivers (Table 1, Fig 3); variation in

345 GPP ranged from 0.6 to 22 g O_2 m^{-2} d^{-1}, and encompassed much of the range of GPP

346 measured previously in small streams. However, for these rivers, unlike many smaller

347 streams, GPP and ER fell closer to the 1:1 line (Fig 3) suggesting that these 14 rivers had

348 low rates of HR relative to GPP. Neither turbidity nor nutrient concentrations correlated

349 with GPP or ER in any of the rivers (Appendix 3). Nearly all Pearson correlation

350 coefficients were < |-0.48|, with corresponding Bayes factor of < 0.9, which provided no

351 support for a linear relationship between the metabolism parameters and potential

352 covariates (Appendix 3). Two exceptions were benthic chlorophyll and total chlorophyll

353 which positively correlated with ER (r=0.76 and 0.78 respectively with Bayes factor >27

354 indicating strong evidence). Log transformed GPP and |ER| were strongly positively

355 correlated with each other (Fig 3, r=0.74, Bayes factor = 18.6).

356   River size affected variation in metabolic rates and GPP/|ER|. GPP and ER were

357 highly variable, but peaked in mid-sized rivers (Fig 4). Estimates of heterotrophic

358 respiration in our 14 rivers spanned a broad range, but were not as high as some streams

359 with <10 m^3 s^{-1} discharge. The ratio GPP/|ER| increased with increasing river size, and

360 large streams and rivers did not have low values of GPP/|ER|. For example, 50% of

15

361 rivers with $Q < 10$ m^3 s^{-1} had GPP/|ER| < 0.3. On the other hand, in rivers with $Q > 10$

362 m^3 s^{-1}, only 14% had GPP/|ER| < 0.3.

363   Gas exchange (K_{600}) varied among the rivers (Table 1), with a mean of 5.7 d^{-1} and

364 a range of 0.5 to 16 d^{-1}; gas exchange rates corresponded to a mean gas exchange velocity

365 (k_{600}) of 20.8 cm h^{-1} with a range of 2 to 71 cm h^{-1}. Gas exchange rate was uncorrelated

366 with river depth, but river depth only varied two-fold among the 14 rivers. River slope

367 strongly predicted gas exchange velocity (Fig 2), and k_{600} fell closely to the prediction

368 estimate based on empirical equations used for many studies (Raymond and others 2012)

369 (Fig 2). The 1:1 prediction line explained 84% of the variation in these 14 rivers relative

370 to the 76% R^2 in Raymond and others (2012).

371   Organic C spiraling lengths (S_{OC}) averaged 319 km and ranged from 38 to 1193

372 km, and S_{OC} lengths were generally similar to their respective river segment lengths;

373 median ratio of S_{OC} to segment length was 1.6 with a range of 0.2 to 4.7 (Table 2). Arid-

374 land rivers with high suspended organic sediment loads and low HR (e.g., Green River at

375 two Utah sites, Colorado River, and Bear River, UT) had much longer S_{OC} than other

376 rivers (Table 2). Mineralization velocities ($v_{f\text{-}OC}$) for the 14 rivers averaged 0.37 m d^{-1} and

377 ranged from 0.05 to 0.81 m d^{-1} and when combined with previous studies, $v_{f\text{-}OC}$ correlated

378 positively with discharge ($r = 0.50$, Bayes factor = 127, strong evidence) (Fig 5).

379

380 **Discussion**

381   Gross primary production and ER varied strongly in our 14 rivers; this variation

382 corresponded to that of other previous measurements in similar-sized rivers. One river,

383 the Henry's Fork, ID had among the highest GPP ever measured for a stream or river.

384   Others, like the Bear River, UT had low rates of metabolism. The 4 rivers in the

385   Midwestern US had moderate rates of metabolism with low variation among them.

386   Despite evidence showing that GPP can increase as a function of stream or river size (Fig

387   4) (Finlay 2011), variation in metabolism among rivers was large enough that rivers have

388   no characteristic rate of metabolism.

389   Because we measured metabolism on only 2 days, during summer baseflow

390   conditions, we did not have a large within-river dataset to examine uncertainty on our

391   estimates. As such, we used a Bayesian method that allowed us to examine parameter

392   error within any one day (Holtgrieve and others 2010). This approach becomes necessary

393   when solving for gas exchange as well as metabolic parameters to avoid equifinality

394   among parameter estimates. In fact, we found low rates of parameter error. Variation

395   among sondes, or between the two measurement days, were higher than error estimated

396   via computational Bayesian approach on any one day, suggesting that these within-day

397   error estimates may not represent day-to-day error well.

398

399   *GPP and ER*

400   GPP ranged widely in our 14 rivers from among the highest rate ever measured

401   (e.g., Henry's Fork) to low rates that were similar to those measured in small, forested

402   streams. Despite this high variability, we were unable to statistically assess controls on

403   variation of GPP among our 14 rivers. Time series of metabolism clearly show that

404   turbidity can control rates of GPP in a river (Hall et al. 2015). We certainly expected that

405   variation in turbidity would control GPP among rivers, but we found only weak

17

406 correlation between GPP and turbidity (Appendix 3), even though variation in turbidity

407 was high, suggesting that some other processes were controlling variation.

408   We acknowledge that we only measured metabolism for two days; it is very likely

409 that antecedent conditions (e.g., time since last flood) may have controlled the rates of

410 GPP that we measured. Variation in the metabolism of one river can be as large as

411 variation among rivers, and a strong role for antecedent conditions has been noted

412 (Uehlinger 2006; Roberts and others 2007; Beaulieu and others 2013). One river, the

413 Muskegon, had an unexpected dam release, tripling discharge the day before our

414 metabolism estimates. This spate may have affected metabolism.

415   Despite these limitations, we can observe some anecdotal evidence for controls on

416 GPP; for example, the rivers with the two highest rates of GPP (Green River, WY and

417 Henry's Fork, ID) were located below water storage impoundments. Rivers below dams

418 typically have stable flow and low turbidity and can have high benthic algal biomass with

419 correspondingly high rates of GPP (Davis and others 2012). Henry's Fork also has

420 substantial inputs of groundwater-fed springs; high metabolism has been measured

421 previously in other spring streams (Odum 1957; Hall and others 2003; Heffernan and

422 Cohen 2010). In contrast, Buffalo Fork, WY drains mountain wilderness and is

423 oligotrophic, and had correspondingly low rates of metabolism. However, we emphasize

424 that we did not design the overall study to statistically tease out controls on river

425 metabolism, but rather to assess rates and variation of riverine nutrient uptake (J. L. Tank

426 and others, unpublished data). Statistically examining controls on metabolism would

427 have required many more rivers (Bernot and others 2010), or we would have selected all

428 rivers along a gradient of a predicted controlling variable, such as nutrient concentrations,

429 in one region of the country.

430   GPP and ER were highly coupled in these 14 rivers (Fig 3), and unlike in some

431 streams, we did not find high riverine ER associated with low rates of GPP. This finding

432 suggests that despite an overall pattern of GPP/|ER| < 1, rivers may not have extremely

433 high rates of HR, at least during baseflow when they are not transporting large amounts

434 of terrestrial C and GPP is high. The relationship between GPP/|ER| as a function of river

435 discharge across the 14 rivers, combined with the full meta-analysis data set, supports

436 this conclusion with small streams having the potential for both low and high ratios of

437 GPP/|ER|, whereas rivers > 10 m^3 s^{-1} had GPP/|ER| > 0.3 in 85% of the observations.

438 Higher rates of GPP in rivers have been previously noted in other meta-analyses of

439 stream metabolism, with the interesting twist that human perturbation has a stronger

440 effect on metabolism in small streams relative to rivers (Finlay 2011). Studies that

441 measure metabolism within a river network have found a similar pattern of increasing

442 GPP/|ER| with downstream position in the network (Meyer and Edwards 1990;

443 McTammany and others 2003); increasing GPP/|ER| with river size could be due to

444 increasing GPP, decreasing HR, or both.

445   Theory predicts that lower rates of HR should occur in downstream reaches

446 because most terrestrial (i.e., allochthonous) OC inputs are mineralized in the headwaters

447 (Webster 2007), yet HR peaks in middle river discharge (Fig. 4). Rather, rivers tended to

448 have high rates of ER, but do not have the negligible rates of GPP found frequently in

449 small, often shaded, headwater streams (Fig. 4). Alternatively, the pattern of somewhat

450 lower HR in larger rivers may be an artifact of the rivers and time chosen for metabolism

451 estimates. Rivers occupying a floodplain may have large spikes in HR during flooding

452 periods (Colangelo 2007; Dodds and others 2013), which are notably not included in the

453 14 estimates of river metabolism that we present here. In addition, as shown by Meyer

454 and Edwards (1990), rivers with large quantities of terrestrially-derived DOC may have

455 high rates of ER relative to GPP, though we note that they too found a pattern of

456 increasing GPP/|ER| with increasing stream order.

457   Many small streams had |ER|>>GPP; but we suggest that it is not possible to have

458 GPP>>|ER| because of a necessary upper limit to GPP/|ER|. For example, high rates of

459 GPP will result in higher ER because of the combination of associated respiration of the

460 autotrophs along with heterotrophic organisms contained in stream biofilms. The fraction

461 of GPP that is autotrophic respiration (AR) will determine this upper limit; given a mean

462 fraction of GPP respired each day (AR_f) of 0.44 (Hall and Beaulieu 2013), we calculate

463 that GPP/|ER| = GPP/(GPP×0.44) = 2.2. Thus we predict that the upper limit of

464 GPP/|ER| is 2.2 because, on average, 44% of GPP constitutes daily autotrophic

465 respiration. Indeed only 1.1 % of GPP/|ER| values exceeded 2.2, suggesting that this

466 value may represent an upper bound for autotrophy in rivers.

467

468 *Gas exchange*

469   The 14 rivers had variable gas exchange and river slope was the primary predictor

470 of gas exchange velocity (k_{600}, Fig. 2); gas exchange was lowest in Bear River, UT which

471 had gas exchange similar to a low-wind lake (Cole and Caraco 1998). Gas exchange was

472 highest in the Henry's Fork, which at 71 cm h^{-1} approached that of the steep, whitewater

473 section of the Colorado through Grand Canyon (Hall and others 2012). The slope of the

474 regression line between river slope and k_{600} was lower for these 14 rivers than for

475 multiple measurements in the Colorado River in Grand Canyon (Hall et al. 2012), likely

476 due to the broad range of reaches through the Grand Canyon, ranging from nearly still to

477 extremely turbulent rapids. Our 14 rivers here did not display this within-river variation

478 in river morphology, even for the pool-drop section of the Green River in Gray Canyon.

479 Nevertheless, gas exchange predicted using empirical equations matched closely with our

480 data, even more closely than the original data used to derive these equations (Raymond

481 and others 2012).

482　　　　There is much interest in understanding gas exchange in rivers to estimate global

483 gas fluxes (Raymond and others 2013). With this study, we show that across a few

484 medium-sized continental rivers, gas exchange can vary widely. For the purposes of an

485 accurate metabolism estimate, it is necessary to estimate gas exchange for each river

486 because the log–log relationship in Fig. 2 has 2-fold prediction error. Optimistically,

487 with high GPP and low rates of O_2 turnover (K_{600}), it is possible to model gas exchange

488 using solely O_2 data, with no need to perform an experimental gas tracer addition (e.g.,

489 SF_6) in these rivers. For the purposes of scaling gas exchange, where it is impractical to

490 empirically measure gas exchange for an entire river network, the method employed by

491 Raymond et al. (2012) is likely the best available for these medium-sized rivers in the

492 sense that it is unbiased (though with large prediction error) and captures much of the

493 variability in k_{600}.

494

495 *C spiraling*

496   Spiraling lengths for OC were generally long, but variable, in these 14 rivers. In 7

497   cases S_{OC} was shorter than the length of the river segment that we measured, suggesting

498   that there can be complete turnover of the OC pool along the length of some rivers.

499   Functionally, rivers with an S_{OC} roughly equal to segment length have turned over > 50%

500   of the OC pool in that length, although a caveat to this conclusion is that we evaluated

501   these rivers at baseflow discharge. High flows associated with storms or snowmelt would

502   assuredly result in much longer OC spiraling lengths because the OC flux would increase

503   more than any increase in organic matter processing (i.e., HR) during high flow periods.

504   Notably, the singular aspect of C cycling that most C spiraling studies (ours and others)

505   generally overlook is that most OC transport will occur during periods of high flow,

506   resulting in substantial intra-annual variation in S_{OC} (Meyer and Edwards 1990).

507   However, our analysis shows that, at least at baseflow, heterotrophic activity can drive

508   substantial mineralization of OC along a river's length. Given scaling relationships

509   between element spiraling length and river length, a constant $v_{f\text{-}OC}$ means that spiraling

510   length increases less than proportionally with downstream distance from headwaters

511   (Hall and others 2013). We suggest that OC mineralization and subsequent turnover of

512   OC pools occurs to the same degree in larger streams and rivers as in the more well-

513   studied small streams.

514   It is important to note that although GPP/|ER| is higher in rivers than headwaters,

515   it is clear that there is substantial processing of allochthonous C in rivers supported by the

516   high rates of HR across a range of stream and river sizes (Fig. 4). This point has also been

517   noted previously by Cole and Caraco (2001) for large rivers; these findings suggest that

518   rivers are important sites for the mineralization for OC. Alternatively this

519 "allochthonous" C fueling excess ER downstream could be C produced via

520 autochthonous production that is subsequently transported, and then mineralized, in

521 downstream river segments (Genzoli and Hall in revision).

522   From the perspective of C cycling, data from these 14 rivers combined with that

523 from the literature support that rivers are reactive ecosystems. With the current interest in

524 examining how freshwater ecosystems contribute to regional and global C budgets

525 (Battin and others 2008; 2009; Raymond and others 2013), we suggest that rivers may

526 strongly influence mineralization and fixation of new C in addition to their more obvious

527 role in the longitudinal transport of C. In fact at baseflow, mineralization and transport

528 are balanced such that OC can turn over completely in some river reaches. In rivers

529 without substantial groundwater inputs containing terrestrial sources of dissolved CO_2,

530 we may expect that net ecosystem production (NEP) for rivers will roughly equal CO_2

531 emissions, as has been found for the Hudson River (Cole and Caraco 2001). Metabolism

532 and C spiraling data from this study represent an approach to examine the

533 biogeochemical mechanisms controlling riverine C cycling, but only represent a snapshot

534 in time. In the future, we expect that time series of metabolism data will provide

535 estimates across a range of seasonal and hydrologic conditions, supporting a more

536 thorough understanding of the role of rivers in C cycling.

537

550

551

References

553 Battin T, Kaplan L, Findlay S, Hopkinson C, Marti E, Packman A, Newbold J, Sabater F.
554   2008. Biophysical controls on organic carbon fluxes in fluvial networks. Nature
555   Geoscience 1:95–100.

556 Battin TJ, Luyssaert S, Kaplan LA, Aufdenkampe AK, Richter A, Tranvik LJ. 2009. The
557   boundless carbon cycle. Nature Geoscience 2:598–600.

558 Beaulieu JJ, Arango CP, Balz DA, Shuster WD. 2013. Continuous monitoring reveals
559   multiple controls on ecosystem metabolism in a suburban stream. Freshwater
560   Biology 58:918–37.

561 Bernot MJ, Sobota DJ, Hall RO, Mulholland PJ, Dodds WK, Webster JR, Tank JL,
562   Ashkenas LR, Cooper LW, Dahm CN, Gregory SV, Grimm NB, Hamilton SK,
563   Johnson SL, McDowell WH, Meyer JL, Peterson BJ, Poole GC, Valett HM, Arango
564   CP, Beaulieu JJ, Burgin AJ, Crenshaw C, Helton AM, Johnson LT, Merriam J,
565   Niederlehner BR, O'Brien JM, Potter JD, Sheibley RW, Thomas SM, Wilson K.
566   2010. Inter-regional comparison of land-use effects on stream metabolism.
567   Freshwater Biology 55:1874–90.

24

568 Chapra SC, Di Toro DM. 1991. Delta method for estimating primary production,
569   respiration, and reaeration in streams. Journal of Environmental Engineering
570   117:640–55.

571 Colangelo DJ. 2007. Response of river metabolism to restoration of flow in the
572   Kissimmee River, Florida, USA. Freshwater Biology 52:459–70.

573 Cole JJ, Caraco NF. 1998. Atmospheric exchange of carbon dioxide in a low-wind
574   oligotrophic lake measured by the addition of SF_6. Limnology and Oceanography
575   43:647–56.

576 Cole JJ, Caraco NF. 2001. Carbon in catchments: connecting terrestrial carbon losses
577   with aquatic metabolism. Marine and Freshwater Research 52:101–10.

578 Cross WF, Baxter CV, Rosi-Marshall EJ, Hall RO, Kennedy TA, Donner KC, Wellard
579   Kelly HA, Seegert SEZ, Behn KE, Yard MD. 2013. Food-web dynamics in a large
580   river discontinuum. Ecological Monographs 83:311–37.

581 Davis CJ, Fritsen CH, Wirthlin ED, Memmott JC. 2012. High rates of primary
582   productivity in a semi-arid tailwater: implications for self-regulated production. River
583   Research and Applications 28:1820–9.

584 Dodds WK, Veach AM, Ruffing CM, Larson DM. 2013. Abiotic controls and temporal
585   variability of river metabolism: multiyear analyses of Mississippi and Chattahoochee
586   River data. Freshwater Science 32:1073–87.

587 Finlay J. 2011. Stream size and human influences on ecosystem production in river
588   networks. Ecosphere 2:87.

589 Griffiths NA, Tank JL, Royer TV, Warrner TJ, Frauendorf TC, Rosi-Marshall EJ, Whiles
590   MR. 2012. Temporal variation in organic carbon spiraling in Midwestern agricultural
591   streams. Biogeochemistry 108:149–69.

592 Genzoli LA, Hall RO. In revision. Shifts in Klamath River metabolism following a
593   reservoir cyanobacterial bloom. Freshwater Science.

25

594   Hall RO, Baker MA, Rosi-Marshall EJ, Tank JL. 2013. Solute specific scaling of

595   inorganic nitrogen and phosphorus uptake in streams. Biogeosciences 10:7323–31.

596   Hall RO, Beaulieu JJ. 2013. Estimating autotrophic respiration in streams using daily

597   metabolism data. Freshwater Science 32:507–16.

598   Hall RO, Kennedy TA, Rosi-Marshall EJ. 2012. Air-water oxygen exchange in a large

599   whitewater river. Limnology and Oceanography: Fluids and Environments 2:1–11.

600   Hall RO, Tank JL, Dybdahl M. 2003. Exotic snails dominate nitrogen and carbon cycling

601   in a highly productive stream. Frontiers in Ecology and the Environment 1:407–11.

602   Hall RO, Yackulic CB, Kennedy TA, Yard MD, Rosi-Marshall EJ, Voichick N, and

603   Behn KE. 2015. Turbidity, light, temperature, and hydropeaking control daily

604   variation in primary production in the Colorado River, Grand Canyon. Limnology

605   and Oceanography 60: 512-26.

606   Heffernan JB, Cohen MJ. 2010. Direct and indirect coupling of primary production and

607   diel nitrate dynamics in a subtropical spring-fed river. Limnology and Oceanography

608   55:677–88.

609   Holtgrieve GW, Schindler DE, Branch TA. 2010. Simultaneous quantification of aquatic

610   ecosystem metabolism and reaeration using a Bayesian statistical model of oxygen

611   dynamics. Limnology and Oceanography 55:1047–63.

612   Hornberger GM, Kelly MG. 1975. Atmospheric reaeration in a river using productivity

613   analysis. Journal of the Environmental Engineering Division 101:729–39.

614   Huryn AD, Benstead JP, Parker SM. 2014. Seasonal changes in light availability modify

615   the temperature dependence of ecosystem metabolism in an arctic stream. Ecology

616   95: 2826-2839.

617   Jähne B, Haußecker H. 1998. Air-water gas exchange. Annual Review of Fluid

618   Mechanics 30:443–68.

619   Jankowski K, Schindler DE, Lisi PJ. 2014. Temperature sensitivity of community

620   respiration rates in streams is associated with watershed geomorphic features.

621   Ecology 95:2707–14.

622   Marcarelli AM, Baxter CV, Mineau MM, Hall RO. 2011. Quantity and quality: unifying

623   food web and ecosystem perspectives on the role of resource subsidies in freshwaters.

624   Ecology 92:1215–25.

625   McTammany ME, Webster JR, Benfield EF, Neatrour MA. 2003. Longitudinal patterns

626   of metabolism in a southern Appalachian river. Journal of the North American

627   Benthological Society 22:359–70.

628   Meyer JL, Edwards RT. 1990. Ecosystem metabolism and turnover of organic carbon

629   along a blackwater river continuum. Ecology 71:668–77.

630   Newbold JD, Mulholland PJ, Elwood JW, O'Neill RV. 1982. Organic carbon spiralling in

631   stream ecosystems. Oikos 38:266–72.

632   Odum HT. 1957. Trophic structure and productivity of Silver Springs, Florida.

633   Ecological Monographs 27:55–112.

634   R Development Core Team. 2011. R: A language and environment for statistical

635   computing. Vienna: R Foundation for Statistical Computing http://www.R-

636   project.org/

637   Raymond PA, Hartmann J, Lauerwald R, Sobek S, McDonald CP, Hoover M, Butman D,

638   Striegl R, Mayorga E, Humborg C, Kortelainen P, Dürr H, Meybeck M, Cais P, Guth

639   P. 2013. Global carbon dioxide emissions from inland waters. Nature 503:355–9.

640   Raymond PA, Zappa CJ, Butman D, Bott TL, Potter J, Mulholland P, Laursen AE,

641   McDowell WH, Newbold D. 2012. Scaling the gas transfer velocity and hydraulic

642   geometry in streams and small rivers. Limnology and Oceanography: Fluids and

643   Environments 2:41–53.

644   Reichert P, Uehlinger U, Acuña V. 2009. Estimating stream metabolism from oxygen

645 concentrations: Effect of spatial heterogeneity. Journal of Geophysical Research

646 Biogeosciences 114:G03016.

647 Roberts BJ, Mulholland PJ, Hill WR. 2007. Multiple scales of temporal variability in

648 ecosystem metabolism rates: results from 2 years of continuous monitoring in a

649 forested headwater stream. Ecosystems 10:588–606.

650 Roley, SS, Tank JL, Griffiths NA, Hall RO, Davis RT. 2014. The influence of floodplain

651 restoration on whole-stream metabolism in an agricultural stream: insights from a

652 5-year continuous dataset. Freshwater Science 33:1043-1059.

653 Staehr PA, Baastrup-Spohr L, Sand-Jensen K, Stedmon C. 2012. Lake metabolism scales

654 with lake morphometry and catchment conditions. Aquatic Sciences 74:155–69.

655 Taylor BW, Flecker AS, Hall RO. 2006. Loss of a harvested fish species disrupts carbon

656 flow in a diverse tropical river. Science 313:833–6.

657 Thomas S, Royer T, Snyder E, Davis J. 2005. Organic carbon spiraling in an Idaho river.

658 Aquatic Sciences 67:424–33.

659 Thorp JH, Delong MD. 2002. Dominance of autochthonous autotrophic carbon in food

660 webs of heterotrophic rivers. Oikos 96:543–50.

661 Tranvik LJ, Downing JA, Cotner JB, Loiselle SA, Striegl RG, Ballatore TJ, Dillon P,

662 Finlay K, Fortino K, Knoll LB. 2009. Lakes and reservoirs as regulators of carbon

663 cycling and climate. Limnology and Oceanography 54:2298–314.

664 Trexler JC, Travis J. 1993. Nontraditional regression analyses. Ecology:1629–37.

665 Uehlinger U. 2006. Annual cycle and inter-annual variability of gross primary production

666 and ecosystem respiration in a floodprone river during a 15-year period. Freshwater

667 Biology 51:938–50.

668 Van de Bogert MC, Carpenter SR, Cole JJ, Pace ML. 2007. Assessing pelagic and

669 benthic metabolism using free water measurements. Limnology and Oceanography:

670 Methods 5:145–55.

671 Vannote RL, Minshall GW, Cummins KW, Sedell JR, Cushing CE. 1980. The river
672   continuum concept. Canadian Journal of Fisheries and Aquatic Sciences 37:130–7.

673 Webster JR. 2007. Spiraling down the river continuum: stream ecology and the U-shaped
674   curve. Journal of the North American Benthological Society 26:375–89.

675 Wetzels R, Wagenmakers E-J. 2012. A default Bayesian hypothesis test for correlations
676   and partial correlations. Psychonomic Bulletin and Review 19:1057–64.

677

678 Table 1. Physical and chemical properties and metabolism of the 14 rivers in this study. Values in parentheses represent 95%

679 bootstrap confidence intervals for metabolism based on 2 to 8 metabolism estimates at each site.

River	Discharge	Width	Velocity	Mean depth	NH_4^+	NO_3^-	SRP	Turbidity	GPP	ER	K_{600}
	$m^3\,s^{-1}$	m	$m\,min^{-1}$	m	$\mu g\,N\,L^{-1}$	$\mu g\,N\,L^{-1}$	$\mu g\,P\,L^{-1}$	fnu	$g\,O_2\,m^{-2}\,d^{-1}$	$g\,O_2\,m^{-2}\,d^{-1}$	d^{-1}
Buffalo Fork	19.1	35.2	55.8	0.58	5	3	44	3	0.8 (0.7, 0.8)	-3.4 (-3.5, -3.3)	8.7 (8.5, 8.9)
Green River, WY	25.5	62.5	32.4	0.76	5	15	21	3	19.9 (18.3, 21.5)	-17.5 (-20.0, -15.0)	8.3 (6.5, 10.0)
Henry's Fork	69.6	62.0	61.7	1.09	3	6	16	1	22.1 (20.6, 23.6)	-18.1 (-20.2, -15.9)	15.6 (13.9, 17.3)
Snake River	71.7	65.3	63.4	1.04	5	bd	7	0	3.0 (2.9,3.1)	--5.1 (-5.6, -4.7)	7.0 (7.0,7.0)
Salmon River	25.9	50.5	59.2	0.52	5	2	4	2	4.0 (3.9,4.2)	-5.1, (-5.8, -4.7)	15.2 (14.2, 16.4)
Tippecanoe River	19.0	50.6	37.9	0.59	15	1850	67	17	2.6 (2.5, 2.7)	-5.3 (-5.4, -5.2)	2.1 (2.0, 2.3)
East Fork, White River	14.0	47.9	21.4	0.82	1	1650	60	43	4.7 (4.4, 5.0)	-5.6 (-5.6,-5.5)	1.7 (1.6, 1.8)
Muskegon River	33.0	67.0	28.3	1.05	14	330	9	23	3.0 (3.0, 3.0)	-4.8 (-4.8, -4.7)	3.0 (3.0, 3.1)
Manistee River	36.5	52.5	33.4	1.25	30	120	10	3	3.9 (3.5,4.2)	-4.4 (-4.6, -4.2)	2.0 (1.9, 2.1)
North Platte River	83.9	81.3	58.9	1.05	5	20	20	19	4.0 (3.7,4.5)	-6.8 (-7.6, -6.1)	4.4 (4.0, 4.9)
Bear River	16.0	37.3	26.6	0.97	12	49	18	53	1.1 (1.0,1.3)	-1.1, (-1.6, -0.7)	0.5 (-0.5,1.6)
Green River at Ouray	37.9	111.8	31.6	0.64	2	7	3	16	1.1 (1.1,1.2)	-1.2, (-1.5, -1.0)	2.1(1.7, 2.6)
Green River at Gray Canyon	41.0	79.1	23.2	1.34	14	19	22	607	0.3 (0.2, 0.5)	-3.0 (-3.1, -2.9)	2.1 (2.0, 2.2)
Colorado River	63.4	83.1	34.3	1.33	1	697	12	116	4.5 (4.3, 4.8)	-2.7 (-3.3, -2.2)	6.3 (6.2 ,6.5)

681 Table 2. Parameters for estimating C spiraling length: dissolved organic C concentration (DOC), particulate OC concentration (POC),

682 and heterotrophic respiration (HR). S_{OC} is OC spiraling length, values in parentheses represent 5% to 95% quantiles of a bootstrap

683 distribution from varying HR. Segment length is length of river between major upstream tributaries and larger downstream rivers or

684 lakes. v_{fOC} is the OC mineralization velocity.

River	DOC	POC	HR	S_{OC}	Segment length	v_{fOC}
	g m^{-3}	g m^{-3}	g C m^{-2} d^{-1}	(km)	(km)	m d^{-1}
Buffalo Fork	2.87	0.43	1.2	134 (123, 143)	44	0.351
Green River, WY	3.64	0.39	3.3	43 (25, 112)	103	0.812
Henry's Fork	2.91	1.06	3.1	123 (66, 433)	120	0.787
Snake River	2.53	0.46	1.4	200 (159, 254)	136	0.473
Salmon River	3.03	0.41	1.2	123 (88, 183)	184	0.360
Tippecanoe River	4.32	0.69	1.6	104 (87, 125)	173	0.310
East Fork, White River	1.53	0.43	1.3	38 (27, 59)	246	0.672
Muskegon River	4.9	0.07	1.3	164 (127, 215)	235	0.259
Manistee River	1.74	0.10	1.0	108 (74, 177)	169	0.553
North Platte River	5.27	0.08	1.9	251 (199, 321)	217	0.354
Bear River	4.08	1.08	0.2	814 (508, 1605)	323	0.045
Green River at Ouray	3.09	0.98	0.3	422 (283, 709)	542	0.069
Green River at Gray Canyon	3.48	14.52	1.1	748 (719, 773)	542	0.060
Colorado River	2.98	2.17	0.3	1194 (403, inf)	264	0.055

685   Figure legends

686   Figure 1. Data (thick gray lines) and model fit (thin black line) for 1

687   representative example of the 2 to 8 metabolism model fits for each of the 14 rivers.

688   Each model fitting procedure was based on one day's worth of oxygen data.   Y axis units

689   are % O_2 saturation to facilitate comparison among rivers.

690   Figure 2. Panel A. Gas exchange velocity from O_2 metabolism model (k_{600}, cm h$^-$

691   ^{1}) increased as a function of river slope (%). Line is linear regression, $\log_{10}(k_{600}) = 2.07 +$

692    $0.79 \times \log_{10}(slope)$, $r^2 = 0.89$. Panel B. Modeled gas exchange velocity lies to close to

693   that predicted by model # 7 in (Raymond and others 2012). Line is 1:1.

694   Figure 3. Gross primary production (GPP) versus ecosystem respiration (ER) for

695   our 14 rivers (black points) and other data (gray circles) show high variation among

696   studies. Line is GPP = ER. Axes are log scaled.

697   Figure 4. Gross primary production (GPP, Panel A), Ecosystem respiration (|ER|,

698   Panel B), and GPP / |ER| (Panel C) as a function of river discharge. Black points are the

699   14 rivers from this study, gray are other data. Axes are log scaled. Lines are locally

700   weighted regression with smoothing factor = 0.75, The point far to the right is from the

701   Mississippi river and represents the largest possible size for a North American river

702   (Dodds and others 2013). Because of the zero density in points between the Mississippi

703   River and the second largest river in the data set, we did not fit the regression line to the

704   Mississippi River.

705   Figure 5. Mineralization velocity of organic carbon ($v_{f\text{-}OC}$) was positively

706   correlated with discharge. Gray points are data from other studies, black points are 13

707   rivers in this study. Error bars are the 5% to 95% quantiles of $v_{f\text{-}OC}$ calculated from a

708   bootstrap of heterotrophic respiration (HR) from Hall and Beaulieu (2013). This error

709   represents uncertainty in HR estimates. Pearson correlation (r= 0.5) and Bayes factor

710   (127) support strong evidence for a positive relationship.
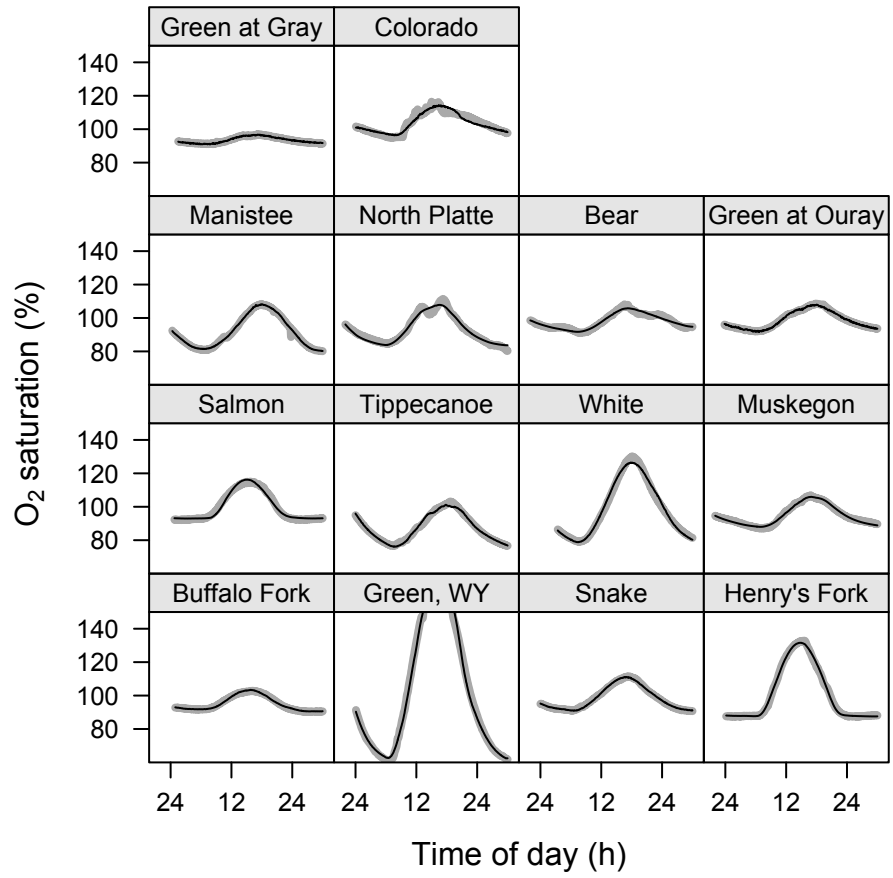
711

712

713

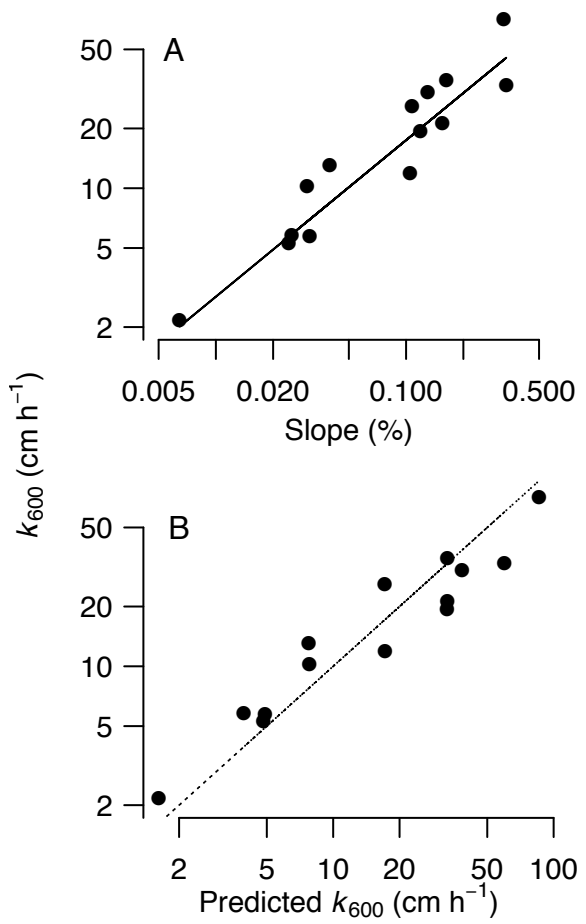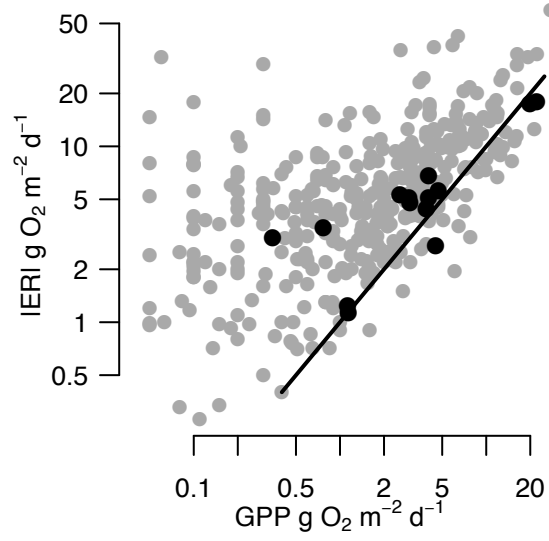714

715

716

717

718

719

720
721
722

723
724
725
726   Fig. 1
727
728
729
730

731
732
733
734
735   Fig 2
736
737
738

739
740
741
742
743   Fig 3
744
745

746
747
748
749
750   Fig 4
751
752
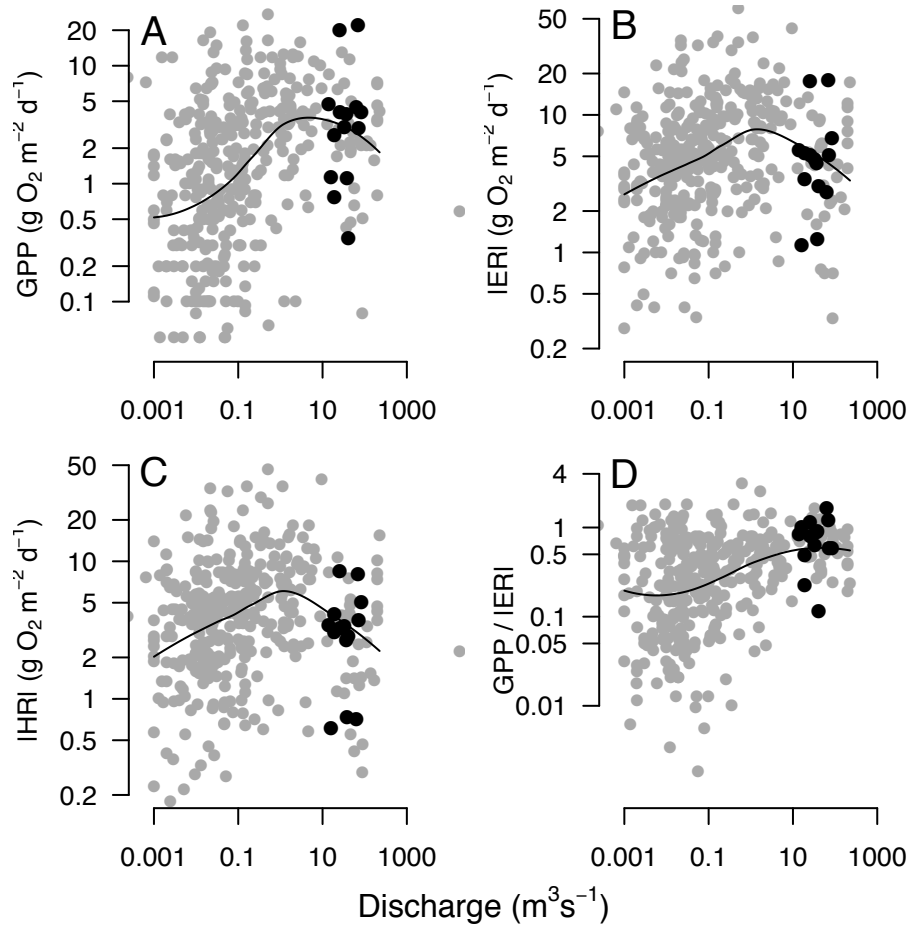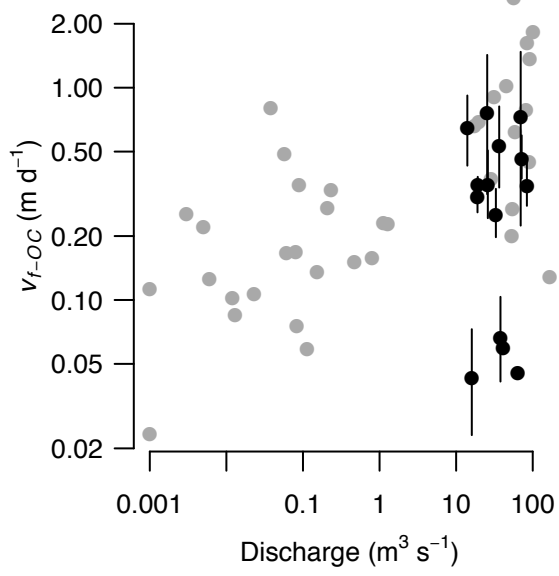
Appendix 1. River physical data.

| River	latitude	longitude	Reach length km	Discharge m³ s⁻¹	Width m	Velocity m min⁻¹	Mean depth m	slope m/m	temp °C	k_{600} cm h⁻¹
Buffalo Fork	43° 50' 57.775" N	110° 19' 39.240" W	10.74	19.1	35.2	55.8	0.58	0.0016	12.0	21.2
Green River, WY	41° 57' 58.508" N	109° 58' 24.282" W	4.34	25.5	62.5	32.4	0.76	0.0011	18.7	26.1
Henry's Fork	44° 6' 14.008" N	111° 20' 55.190" W	8.86	69.6	62.0	61.7	1.09	0.0033	18.6	71.0
Snake River	43° 49' 40.163" N	110° 131' 49.238" W	7.96	71.7	65.3	63.4	1.04	0.0013	16.3	30.3
Salmon River	44° 16' 58.211" N	11° 19' 36.731" W	9.72	25.9	50.5	59.2	0.52	0.0034	16.1	32.9
Tippecanoe River	41° 1' 25.971" N	86° 35' 5.982" W	4.86	19.0	50.6	37.9	0.59	0.0002	26.2	5.2
East Fork, White River	39° 10' 0.043" N	85° 54' 40.264" W	7.41	14.0	47.9	21.4	0.82	0.0003	28.2	5.8
Muskegon River	43° 20' 48.584" N	85° 56' 25.359" W	5.01	33.0	67.0	28.3	1.05	0.0004	24.9	13.1
Manistee River	44° 16' 3.389" N	86° 0' 57.689" W	5.07	36.5	52.5	33.4	1.25	0.0003	22.6	10.4
North Platte River	42° 45' 46.750" N	105° 23' 41.987" W	8.15	83.9	81.3	58.9	1.05	0.0012	23.1	19.3
Bear River	41° 58' 30.905" N	111° 56' 13.003" W	2.50	16.0	37.3	26.6	0.97	0.0001	23.6	2.0
Green River at Ouray	40° 10' 56.773" N	109° 35' 44.690" W	3.97	37.9	111.8	31.6	0.64	0.0003	23.6	5.6
Green River at Gray Canyon	39° 11' 47.847" N	110° 4' 38.751" W	5.25	41.0	79.1	23.2	1.34	0.0011	25.1	11.7
Colorado River	38° 48' 45.218" N	109° 18' 29.116" W	5.15	63.4	83.1	34.3	1.33	0.0016	25.1	35.0

Appendix 2. Error estimates for metabolism parameters
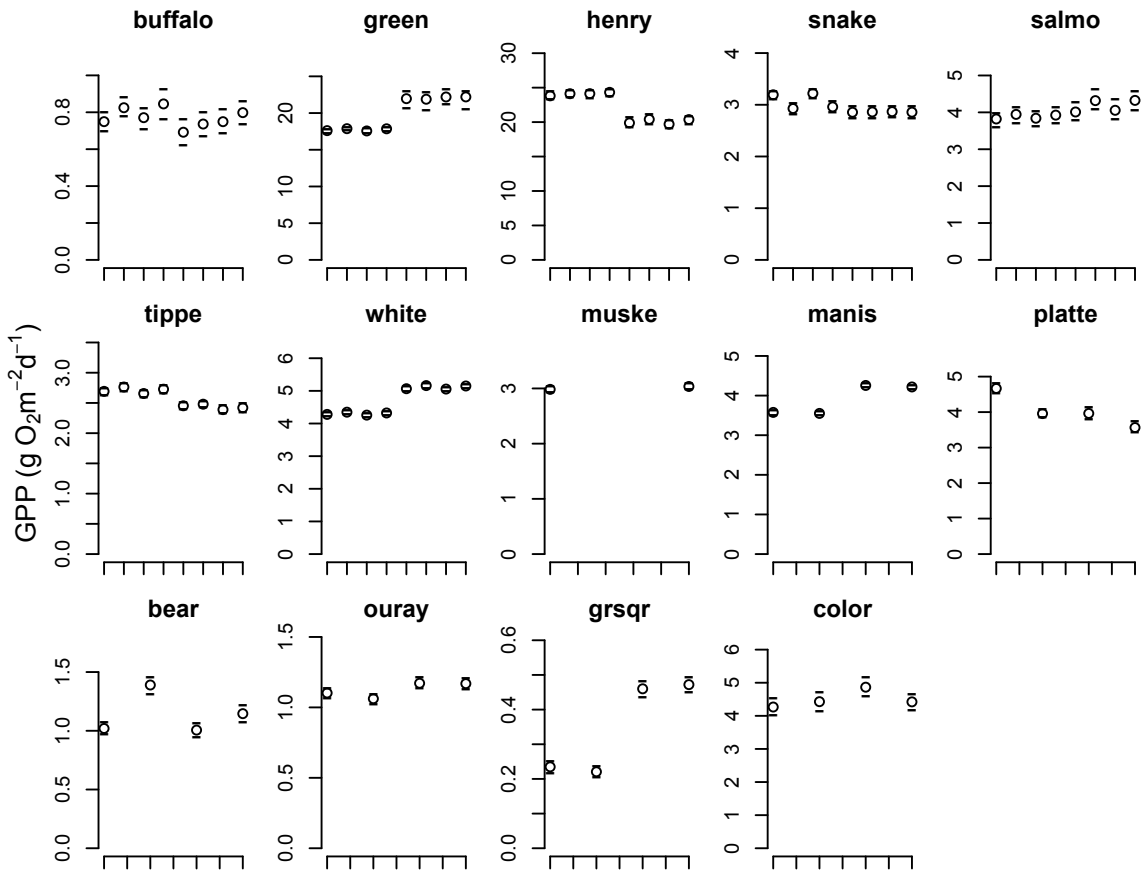
Appendix 2, Figure 1. GPP for 2 to 8 estimates in each of the rivers. Points are median estimate of the posterior probability distribution of the GPP parameter. Line symbols are the 2.5% and 97.5% quantiles of the posterior probability distribution.
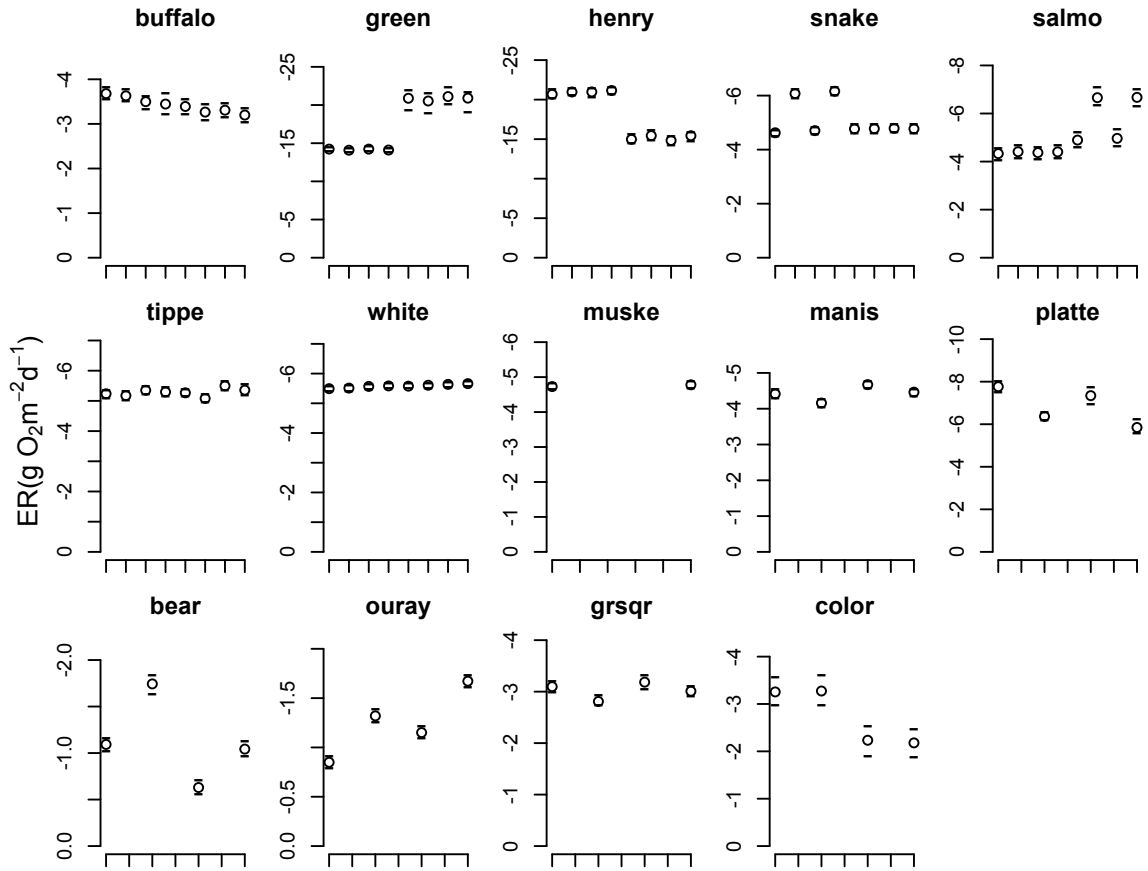
Appendix 2, Figure 2. Ecosystem respiration (ER) for 2 to 8 estimates in each of the rivers. Points are median estimate of the posterior probability distribution of the ER parameter. Line symbols are the 2.5% and 97.5% quantiles of the posterior probability distribution.
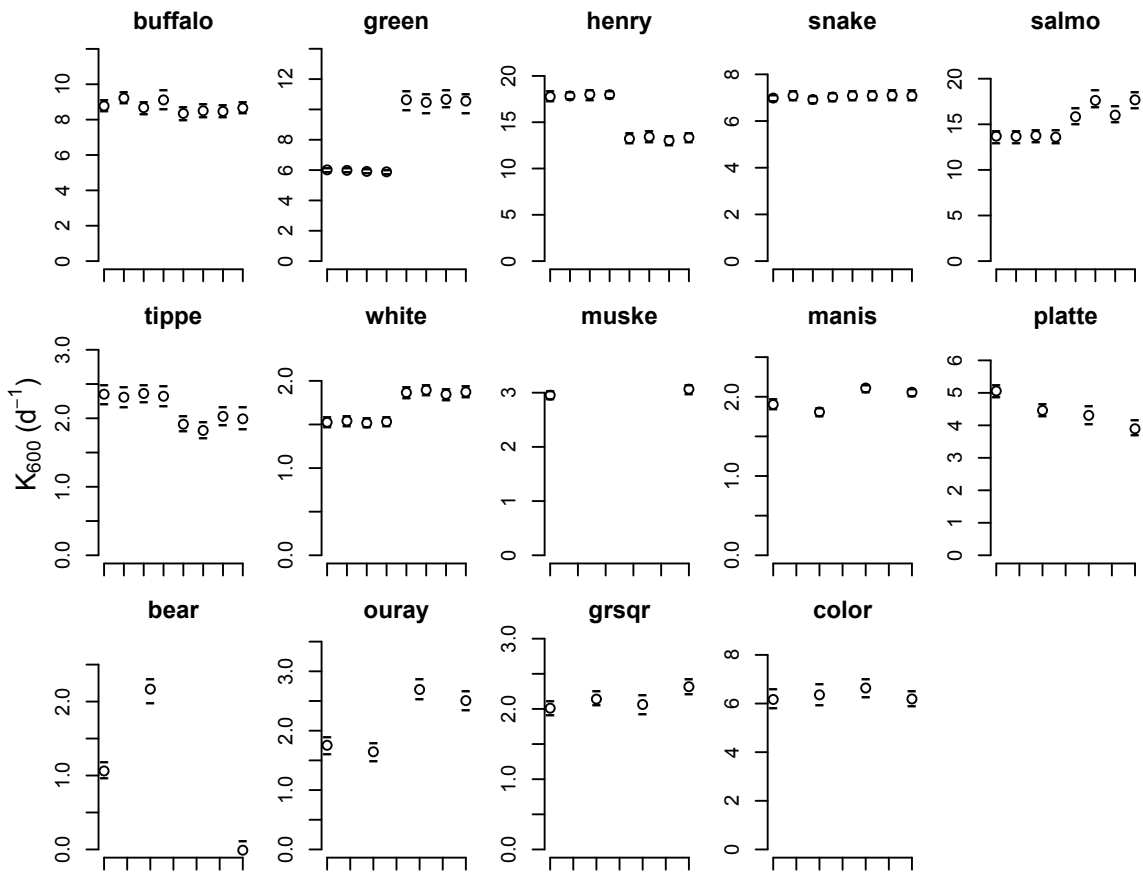
Appendix 2, Figure 3. Gas exchange (K_{600}, d^{-1}) for 2 to 8 estimates in each of the rivers. Points are median estimate of the posterior probability distribution of the K_{600} parameter. Line symbols are the 2.5% and 97.5% quantiles of the posterior probability distribution.

Appendix 3. Pearson correlation coefficients (*r*) between nutrient concentrations, turbidity and metabolism (gpp= gross primary production, er = |ecosystem respiration|). All data except temperature were ln transformed. Bold indicate correlations with strong evidence for a linear relationship (*r* > 0.72 corresponding to Bayes Factor >10 with *n*=14) GPP and |ER| were positively correlated with Bayes factor = 18.6, showing strong evidence for a linear relationship. The only other variable to correlate with metabolism was benthic and total chlorophyll standing stocks.

	er	no3	nh4	srp	turbidity	DOC	pelagic chla	benthic chla	total chla	temp	width
gpp	**0.79**	0.07	-0.28	-0.02	-0.50	-0.12	-0.02	0.48	0.53	-0.10	-0.07
er		-0.08	-0.05	0.25	-0.48	-0.03	-0.17	**0.76**	**0.74**	-0.26	-0.17
no3			-0.01	0.50	0.56	-0.05	**0.83**	0.24	0.32	0.81	-0.11
nh4				0.04	-0.04	0.30	-0.11	0.21	0.21	-0.02	-0.32
srp					0.27	-0.02	0.44	0.36	0.27	0.21	-0.52
turbidity						0.24	0.71	-0.15	-0.10	**0.75**	0.28
DOC							-0.05	0.05	0.15	0.05	0.21
pelagic chla								0.00	0.08	**0.89**	0.08
benthic chla									0.95	-0.09	-0.38
total chla										0.02	-0.29
temp											0.30

Units for this table:
gpp and er (g O_2 m^{-2} d^{-1}), no3 and nh4 (µg N L^{-1}), srp (µg P L^{-1}), turbidity (FNU), DOC (mg C L^{-1}), chla (mg chlorophyll *a* m^{-2}), temp (°C)

Appendix 4. Metabolism data used in meta-analysis. Units are g O_2 m^{-2} d^{-1} for GPP and ER. Q is discharge in L s^{-1}. Table is .csv file.

Appendix 5. R code used to estimate 2 station metabolism via a Bayesian framework.